

Mesozoic Syncollision Siliciclastic Sediments of the Bol'shoi Lyakhov Island (New Siberian Islands)

A. B. Kyz'michev*, A. V. Soloviev*, V. E. Gonikberg*,
M. N. Shapiro**, and O. V. Zamzhitskii*

*Geological Institute, Russian Academy of Sciences, Pyzhevskii per. 7, Moscow, 119017 Russia

**United Institute of Earth Physics, Russian Academy of Sciences,
ul. Bol'shaya Gruzinskaya 10, Moscow, 123995 Russia

Received January 24, 2005

Abstract—Graywackes and shales of the Bol'shoi Lyakhov Island originally attributed to the Mesozoic were subsequently considered based on microfossils as the Late Proterozoic in age. At present, these sediments in the greater part of the island are dated back to the Permian based on palynological assemblages. In the examined area of the island, this siliciclastic complex is intensely deformed and tectonically juxtaposed with blocks of oceanic and island-arc rocks exhumed along the South Anyui suture. The complex is largely composed of turbidites with members displaying hummocky cross-stratification. The studied mineral and geochemical characteristics of the rocks defined three provenances of clastic material: volcanic island arc, sedimentary cover and/or basement of the ancient platform, and exotic blocks of oceanic and island-arc rocks such as serpentinites and amphibolites. All the rock associations represent elements of an orogenic structure that originated by collision of the New Siberian continental block with the Anyui–Svyatoi Nos island arc. Flyschoid sediments accumulated in a foredeep in front of the latter structure in the course of collision. The Late Jurassic volcanics belonging to the Anyui–Svyatoi Nos island arc determine the lower age limit of syncollision siliciclastic rocks. Presence of Late Jurassic zircons in sandstones of the flyschoid sequence in Bol'shoi Lyakhov Island is confirmed by the fission-track dating. The upper age limit is determined by the Aptian–Albian postcollision granites and diorites intruding the siliciclastic complex. Consequently, the flyschoid sequence is within stratigraphic range from the terminal Late Jurassic to Neocomian. It appears that Permian age of sediments suggested earlier is based on redeposited organic remains. The same Late Jurassic–Neocomian age and lithology are characteristic of fossiliferous siliciclastic sequences of the Stolbovoi and Malyy Lyakhov islands, the New Siberian Archipelago, and of graywackes in the South Anyui area in Chukchi Peninsula. All these sediments accumulated in a spacious foredeep that formed in the course the late Cimmerian orogeny along the southern margin of the Arctic continental block.

DOI: 10.1134/S0869593806010035

Key words: New Siberian Islands, Laptev Sea, Arctic region, South Anyui suture, Mesozoic, flysch, fission-track zircon dating.

INTRODUCTION

The Bol'shoi Lyakhov Island (Fig. 1) is largely composed of flyschoid sequence of sandstones, siltstones, and shales. Most extensive rock outcrops are located in the southeastern part of the island (the Khaptagai-Tas, Cape Burus-Tas and nearby areas). Small exposures are also known in the western (Cape Kigilyakh) and northern (Usuk-Yuryakh Rise, Fig. 2) parts of the island. The siliciclastic complex is irregularly deformed, foliated, phyllitized, and intruded by discordant postcollision granodiorite and granite. According to results obtained by K–Ar, Ar–Ar, and U–Pb dating, intrusions are of the Aptian–Albian age (Dorofeev *et al.*, 1999; Vol'nov *et al.*, 1999; Layer *et al.*, 2001; *Placer Deposits...*, 2001)

Northwestward, in the Kotel'nyi and Bel'kovskii islands (Fig. 1), Paleozoic shallow-water carbonate and

siliciclastic rocks are exposed. They constitute a deformed sedimentary cover of an ancient continental block, the New Siberian platform. Upper Jurassic volcanics and graywackes exposed on the Cape Svyatoi Nos southward of the Lyakhov Islands (Fig. 1) are usually considered as rocks of the Anyui–Svyatoi Nos (Svyatoi Nos, Svyatoi Nos–Oloi) island arc (Natal'in, 1984; Parfenov, 1984; Zonenshain *et al.*, 1990; Natal'in *et al.*, 1999; Parfenov *et al.*, 2001; Sokolov *et al.*, 2002). It is universally accepted that the Anyui–Svyatoi Nos island-arc terrane is separated in the present-day structure from the New Siberian platform by the South Anyui suture, a fold–thrust zone several tens of kilometers wide containing ophiolite fragments (Seslavinskii, 1979; Zonenshain *et al.*, 1990). In the Bol'shoi Lyakhov Island, northern termination of the South Anyui suture encloses tectonic slices and wedges of oceanic

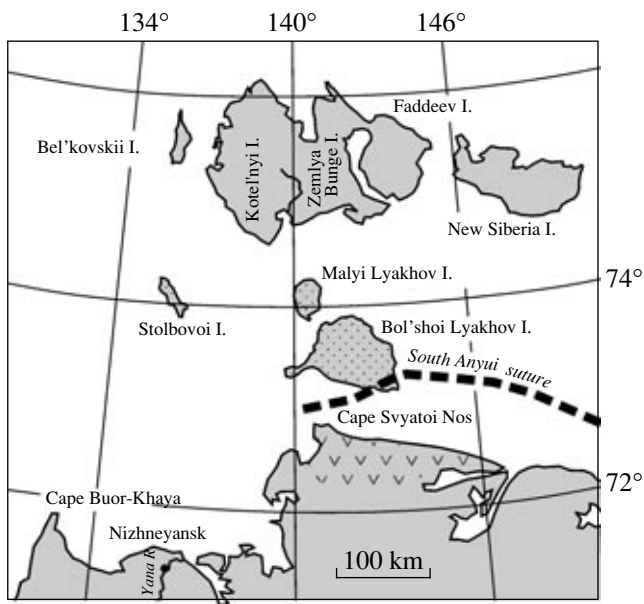


Fig. 1. Schematic map of the study region with shown locations of the South Anyui suture (dashed line), Anyui-Svyatoi Nos arc (ticks), and siliciclastic complex constituting the Lyakhov Islands (dots).

basalts, serpentinites, and amphibolites (Seslavinskii, 1979; Drachev *et al.*, 1993; Vol'nov, 1999).

Views on the age of flyschoid sequence of the Bol'shoi Lyakhov Island repeatedly changed in the course of investigation history. First researchers united all the siliciclastic rocks into a single complex initially attributed to the Mesozoic (Volossovich, 1901; Ermolaev, 1932). After small-scale geological survey of 1956, these sediments were referred to the Upper Proterozoic, because they look older than Paleozoic sequences exposed in northerly islands. The sediments were united into the Burus-Tas Formation named after the eponymous cape in the southern part of the island (Fig. 2). The assumed Late Proterozoic age of rocks was substantiated by the found representative acritarch assemblage (Voitsekhovskii and Sorokov, 1957). Subsequently, the Burus-Tas Formation was studied by V.A. Vinogradov, A.I. Samusin, and their colleagues. They found miospores of Permian age in exposures of the Cape Burus-Tas area (Vinogradov *et al.*, 1974). The palynological assemblage included also some forms characteristic of the Carboniferous, and researchers concluded that the formation is most likely the Permian in age, but did not rule out the Carboniferous age of its

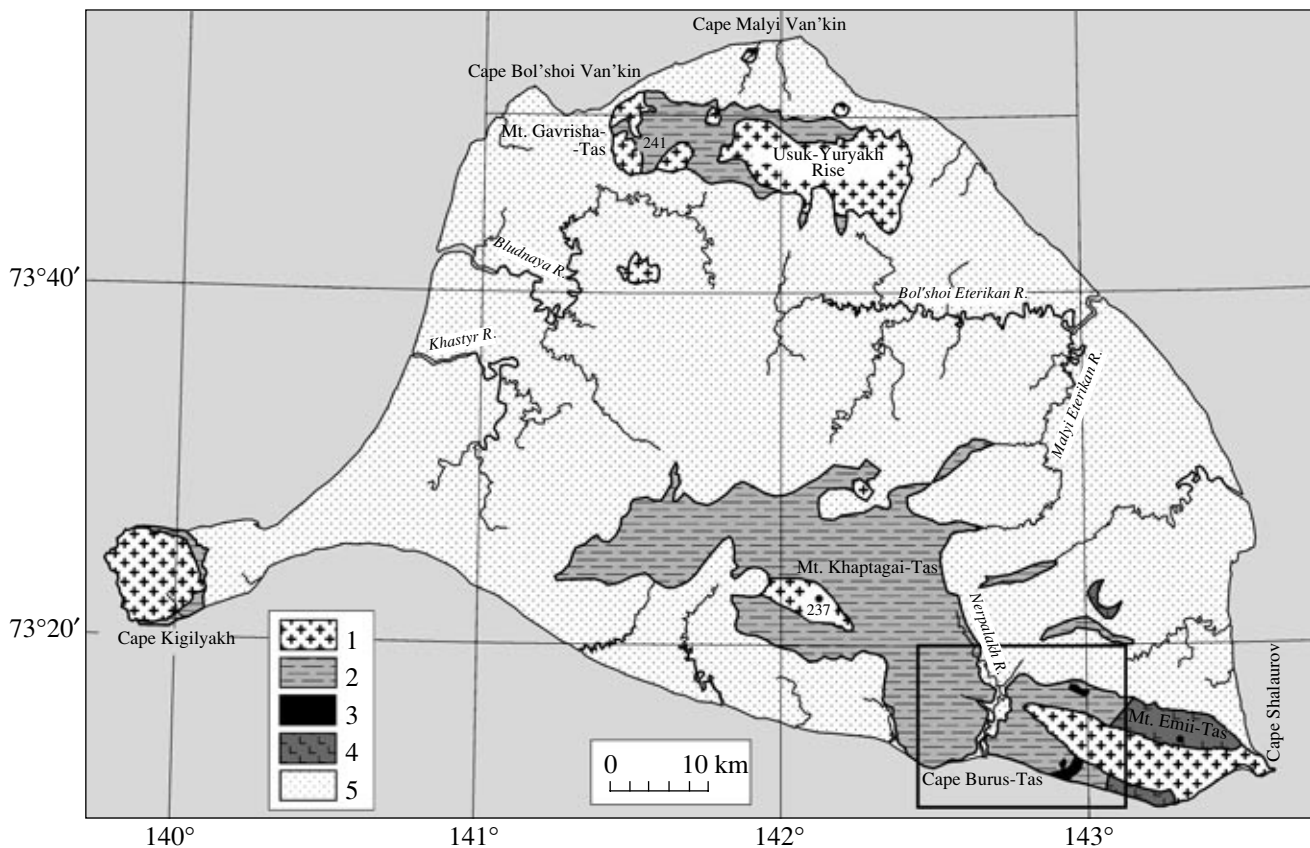


Fig. 2. Geological map of the Bol'shoi Lyakhov Island (compiled using materials from Samusin *et al.*, 1975 and some other works; rectangle designates the area shown in Fig. 3): (1) Cretaceous (Aptian-Albian) granites and diorites; (2) Mesozoic (Volgian-Neocomian): siliciclastic sediments, the Burus-Tas Formation previously referred to the Permian included; (3) serpentinite and associated rocks; (4) amphibolites; (5) non-lithified sediments.

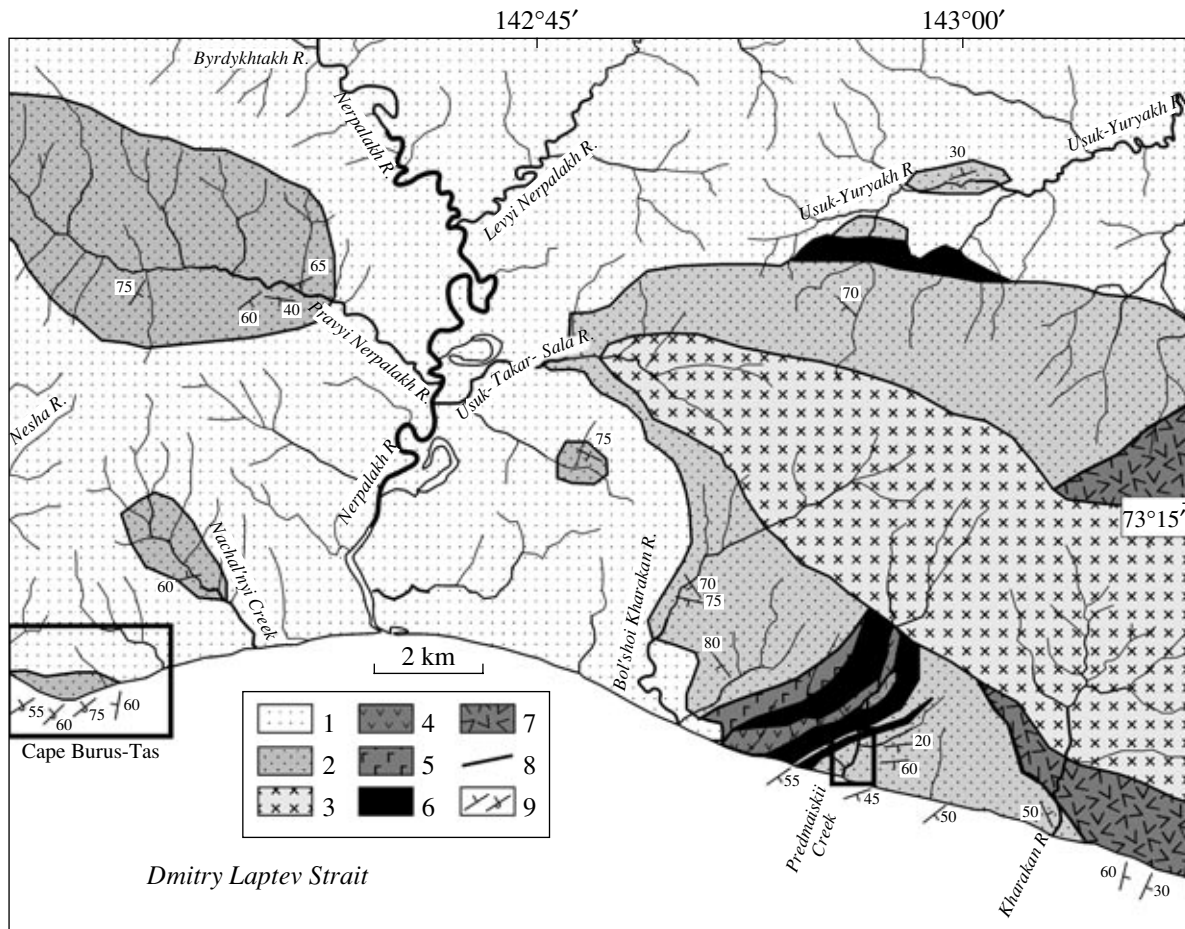


Fig. 3. Geological map of southeastern Bol'shoi Lyakhov Island (rectangles outline the Cape Burus-Tas and Predmaiskii Creek areas of detailed works, which are shown in Figs. 4 and 6): (1) non-lithified sediments (N-Q); (2) Burus-Tas Formation ($J_{3v}-K_1nc$); (3) granodiorites, granites (K_1); (4) spheroidal lavas; (5) gabbro-dolerites; (6) serpentinites; (7) amphibolites; (8) tectonic contacts; (9) bed attitude.

lower part. In 1972–1974, Samusin and his colleagues who carried out geological survey at scale 1 : 200000 in the island excluded siliciclastic sediments of western and northern areas of the island from the Burus-Tas Formation. They showed them on maps as Upper Jurassic rocks (Samusin and Belousov, 1985) by analogy with sequences exposed in neighboring Stolbovoi and Malyi Lyakhov islands, where Volgian bivalves were found by that time (Vinogradov and Yavshits, 1975). Subsequently, during the small-scale cosmic–geological survey of the island in the 1980s, B.N. Aulov and his team dated the Burus-Tas Formation back to the Permian–Triassic (Vol'nov *et al.*, 1999). The Triassic age was substantiated by a bivalve shell of the Triassic affinity found by V.K. Dorofeev in a plate of shale from the Predmaiskii Creek mouth area (Fig. 3). Referring to Samusin, Aulov pointed out that this shell belongs to *Monotis ochotica* (Aulov, 2000, private communication). Based on this find, he referred the formation to the Lower–Middle Triassic and correlated it with coeval sandy–shaly sequences of the Chukchi Peninsula.

In 2000 and 2003, we studied the Burus-Tas Formation in the southeastern part of the island. Continuous rocky exposures were examined in two localities: in the Cape Burus-Tas area and near the Predmaiskii creek mouth (Fig. 3). In the remaining part of the island, there are only separate outcrops along creeks and the Burus-Tas Formation is mapped based on a slightly redeposited alluvium. Our data enable a new interpretation of age and tectonic position of the flyschoid sequence in Bol'shoi Lyakhov Island. In the paper, we show that it accumulated during the terminal Jurassic–Neocomian in a foredeep that developed along southern margin of the New Siberian platform in the course of its collision with the Anyui–Svyatoi Nos island arc.

STRUCTURE OF THE EXAMINED AREA

In the study area (Fig. 3), the Burus-Tas Formation is separated by steep thrust faults from pillow basalts, serpentinites, and amphibolites, which represent fragments of the lithosphere underlying the Jurassic Anyui oceanic basin and Anyui–Svyatoi Nos island arc. It is

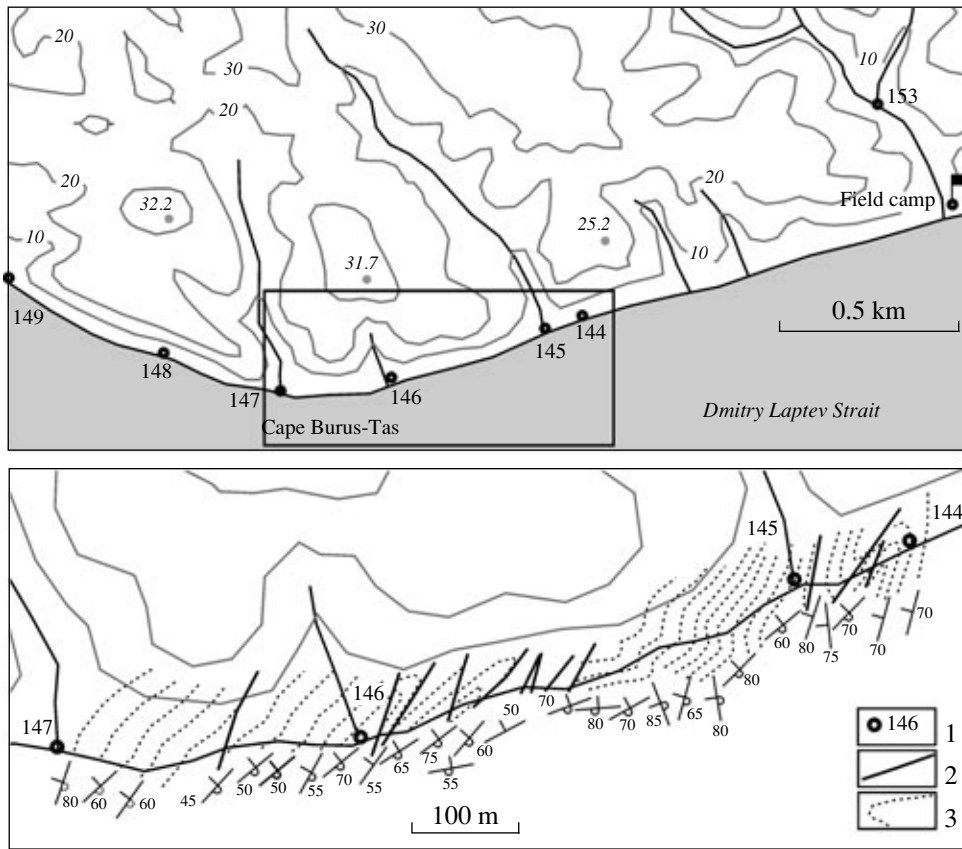


Fig. 4. Schematic location of the Cape Burus-Tas reference section (upper figure) and structure of its examined fragment (semi-closed rectangles in upper map are trigonometric points and altitudes): (1) observation sites and their numbers; (2) faults; (3) interpolated structural lines.

difficult to get insight into structure of the study area, because exposures are fragmentary. In general, structural elements of northwestern vergence extend northeastward that is consistent with thrusting direction of tectonic nappes in the South Anyui suture. Attitude of some beds observed in exposures of the Burus-Tas Formation is sometimes discordant with the regional vergence trend. As is seen in Fig. 3, in some areas the beds are of either northwestern or sublatitudinal strike. We assume that the turns in the strike are explainable in many cases by displacements along strike-slip faults of the northwestern orientation, as is evident from folds with steep hinges observable in exposures. Nevertheless, such an assumption cannot explain all the variants of beds attitude. For example, the Cape Burus-Tas fold structure is of the southeastern vergence untypical of the region in general. Limbs of folds, which are usually overturned in this area, dip northwestward at angles of 50 to 70°. Shales of the Burus-Tas Formation are irregularly phyllitized. The most intense alteration of rocks has been observed in western parts of the examined region, in the Burus-Tas Cape area and in upper reaches of the Nerpalakh River, where cleavage of rocks containing secondary chlorite and sericite is strong.

STRUCTURE OF THE EXAMINED SECTION FRAGMENTS AND SEDIMENTATION SETTING

The Burus-Tas Formation is composed of sandstones, siltstones, and shales. Its lithology is uniform throughout the study area, where dominant fine- to medium-grained sandstones that form beds up to 1.5 m thick alternate with members of bedded shales up to several meters thick. Coarse-grained sandstones, gravelstones, and conglomerates are missing from the examined area, and this suggests that the basin of sedimentation was rather remote from main provenance. Sandstones enclose abundant concretions cemented by carbonate matter. There are members composed predominantly of either sandstone or shale beds. Locally, sandstones and shales are in rhythmical flyschoid alternation. The rocks are mostly gray-colored. Sections of the Cape Burus-Tas and Pravyi Nerpalakh River enclose green sandstones and siltstones. Lilac to green variegated sandstones are observed in the upper reaches of the Nerpalakh River (beyond the presented map). Because of scarce exposures and uniform lithology, we got no success in subdividing the siliciclastic complex, compiling its bed-by-bed section, and estimating thickness. Therefore, position of examined fragments in the whole succession remains unclear. In order to exem-

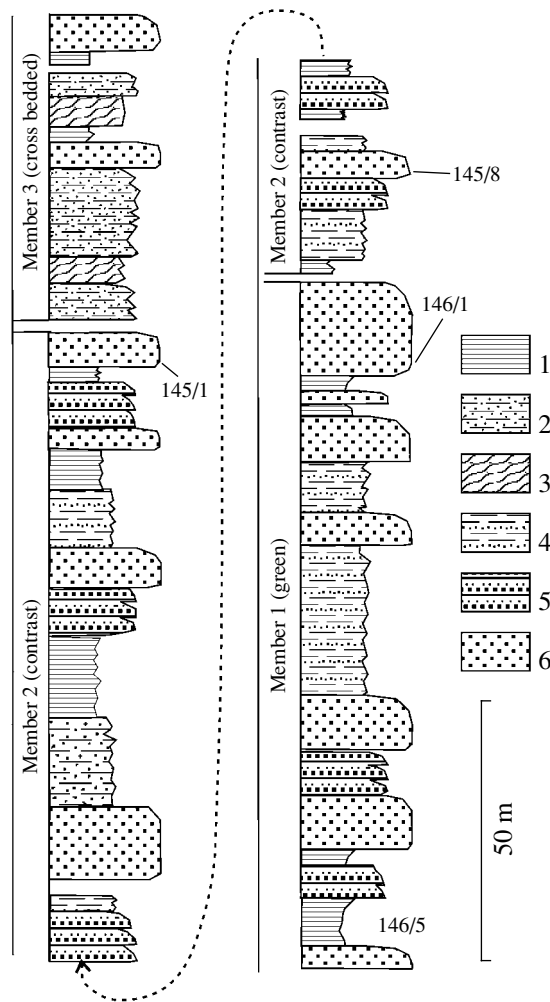


Fig. 5. Structure of the Burus-Tas Formation in the eponymous cape area with samples indicated in Tables 5 and 6, (gaps in columns correspond to largest faults): (1) members with dominant shales and siltstones and thin sandstone interbeds; (2) members with dominant poorly sorted silty sandstones, parallel bedded and obscurely bedded, with intense cleavage; (3) the same with distinct cross bedding; (4) irregularly alternating sandstones, siltstones, and shales; (5) members of rhythmical alternation with well-developed gradational stratification; (6) dominant massive sandstones.

plify the section, we describe two its fragments exposed in the Cape Burus-Tas and Predmaisii Creek mouth area.

The Cape Burus-Tas section (stratotype of the synonymous formation) was previously studied by Vinogradov *et al.* (1974) and by Aulov with colleagues. Their descriptions differ from each other and from results of our observations. According to our data, beds of the Cape Burus-Tas section are overturned, getting younger eastward. A section fragment exposed eastward of the Cape Burus-Tas is studied rather thoroughly. Judging from discontinuous observations, the fragmentary outcrops exposed westward of the cape

and corresponding to a lower part of the section are of uniform lithology. Over a distance of approximately one kilometer east of trigonometric point 144 (Fig. 4), we observed discrete outcrops of dark gray, bedded siltstones and subordinate sandstones partly covered by pebbles. Despite the separated state of outcrops, the general impression is that the upper part of the section is composed predominantly of fine-grained varieties.

For simplification, we describe the section as continuous, although it is interrupted by numerous brecciation zones and some of its fragments are probably truncated by faults. It seems that the section is not doubled, because repeated lithology has not been observed. The reconstructed section is subdivided into three members (Figs. 4, 5).

(1) The “green” member is composed of massive greenish to yellow-green sandstone and less common green siltstone beds. There are members of massive sandstones up to 2 m thick and rhythmically bedded members of sandstones and shales. At least a half of rock in the member is not green, colored gray instead. Locally, sandstones contain abundant concretions of carbonate sandstones up to 20 cm across. Sandstones are green in color because of presence of chlorite flakes, sometimes well visible through a magnifying glass. There are also bright green translucent flakes described during field works as serpentinite. The integral thickness is 100–110 m.

(2) The contrast member includes packets of sandstone-siltstone-shale cyclites with graded bedding in addition to standard gray-colored massive or obscurely bedded sandstones, frequently with concretions, and fine-grained varieties with intense cleavage. The thickness of cyclites is a few meters. There are also siltstone and sandstone beds with asymmetrical ripple marks. The thickness is approximately 160–170 m.

(3) The “cross-bedded” member is dominated by fine-grained rocks with massive sandstone interbeds and poorly sorted obscurely bedded silty sandstones and sandy siltstones. The last variety demonstrates cross bedding at least at two levels of the section. Cross-bedded rocks include up to 7–8 rhythms differently oriented and 3 to 10 cm thick each. Gentle angles of oblique lamination allow interpretation of cross bedding as hummocky cross-stratification (Dott and Bourgeois, 1982). The thickness is 60 m.

The composite thickness of the described section fragment is about 330 m. In total, at least 700 m of the siliciclastic section is exposed in the Cape Burus-Tas area.

Flyschoid members of the Cape Burus-Tas section are typical turbidites with Bouma cycles (Einsele, 1992) more or less expressed. Massive sandstone interbeds usually rest upon the erosion surface. Bedding is obscure or seen only in upper parts of the members when they grade into siltstones. Sometimes, sediments of the transition zone are of gradational type. The mas-

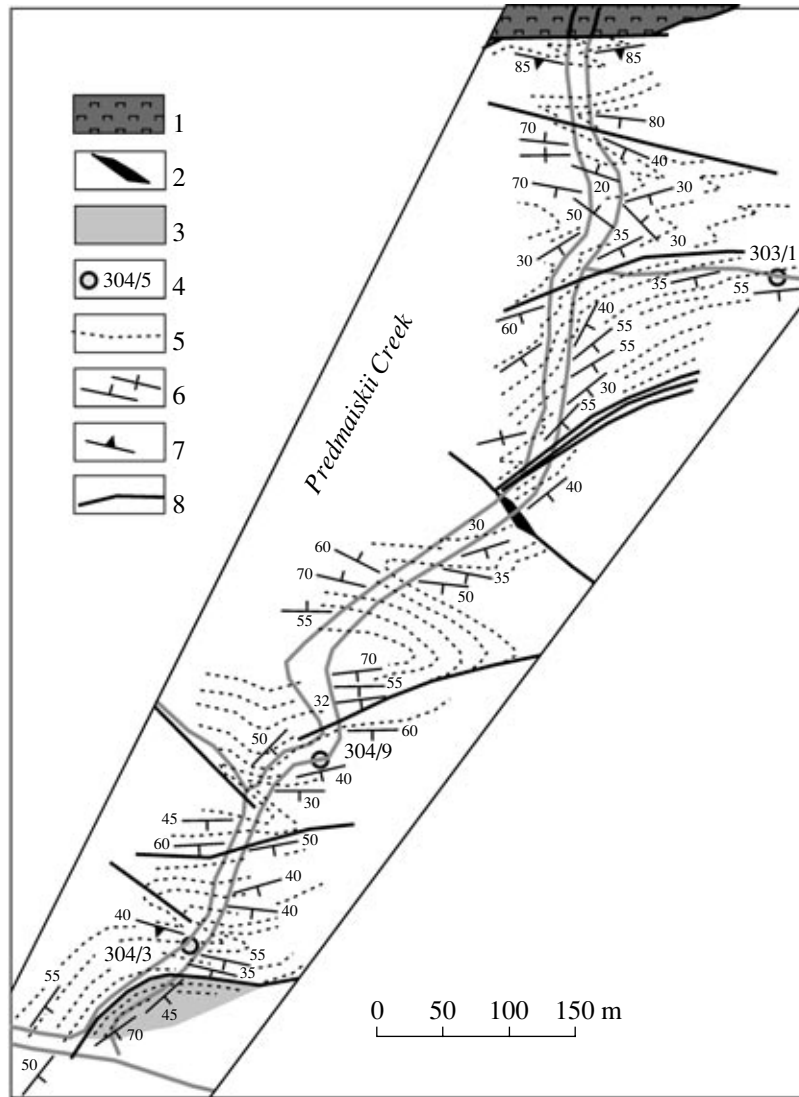


Fig. 6. Schematic structure of the Burus-Tas Formation reference section along the Predmaiskii Creek: (1) serpentinite; (2) granite-porphry; (3) black shale member, which is probably alien for the Burus-Tas Formation; (4) examined samples (Tables 5 and 6); (5) interpolated structural lines; (6) attitude elements of beds; (7) attitude elements of foliation; (8) faults.

sive beds are probably deposited by high-density grain flows. The mentioned character of sedimentation points to a high rate of basin filling with sediment transported from neighboring mountainous (?) land (Mutti *et al.*, 2003), and this was likely responsible for a low content of organic remains in the rocks. Packets of poorly sorted silty sandstones several meters thick, displaying the hummocky cross stratification are important indicators of the paleobasin depth. Such sediments are thought to be depositing in settings several tens meters deep (Dott and Bourgeois, 1982). Their co-occurrence with turbidites suggests that the latter are also shallow-water sediments.

Cleavage in the section of the Burus-Tas Formation nearby the Predmaiskii Creek is poorly developed. The continuous rocky section is exposed for a distance of 300 m along the creek. Separate outcrops occur also

upstream and on the shore of the Dmitry Laptev Strait (Fig. 6). The continuous section is subdivided into four members (from the base upward and downstream):

(1) Sandstones, massive (beds up to 10–50 cm thick), light gray, with thin intercalations of ashy-gray siltstones and spherical or egg-shaped concretions of calcareous sandstones. The sandstones are bedded, with regular, discrete, and lenticular stratification. In upper parts of some layers, there is seen obscure wavy (?) cross bedding. The thickness is 35 m.

(2) The member with more distinct rhythmic alternation of sandstones, siltstones, and shales and with packets (3–6 m thick) of alternating siltstones and shales; in its upper part there is a packet of dominant sandstones approximately 15 m thick. Some sandstone beds with lower erosion boundary show the upward

Table 1. Quantities of detrital grains in five representative sandstone samples from the Burus-Tas Formation

Sample	Qm	Qp	QF	F	P	K	Lv	Ls	Lm	Col	Op	?	Sec	Mtx	SUM
135/1	27	6	–	61	13	4	70	13	2	3	1	4	4	84	200
135/2	72	3	5	56	12	7	107	26	10	1	1	4	19	126	300
145/8	42	4	2	48	12	–	150	29	12	6	–	6	19	107	305
146/1	71	14	3	72	13	9	71	11	22	9	5	8	6	106	300
304/3	59	4	2	69	4	–	117	26	14	3	2	5	4	126	300

Note: (Qm) monocrystalline quartz; (Qp) polycrystalline quartz; (QF) intergrowths of quartz with feldspar; (F) feldspars undivided; (P) plagioclases; (K) potash feldspar; (Lv, Ls, Lm) grains of volcanic, sedimentary, and metamorphic rocks; (Col) colored minerals; (Op) ore minerals; (SUM) sum of points in diagnosed detrital grains.

lithologic succession typical of turbidites: basal massive sandstone grades via bedded variety into lenticular-bedded sandstone and then into siltstone and shale. Some sandstone beds are variably thick and locally pinch out in the exposure. The member thickness is 70 m.

(3) The member similar to the underlying one though dominated by siltstones and shales; Bouma cycles typical of turbidite are distinguishable in some layers. The cycles include (a) massive sandstone with straight gradational stratification, sharp erosional lower boundary, and rip-up argillite clasts in the lower part (40–50 cm); (b) parallel-bedded sandstone (5–10 cm), (c) cross-bedded silty sandstone (5 cm), (d) alternating parallel-bedded siltstone and shale (10 cm), (e) black shale (5 cm). Some siltstone and sandstone interbeds are characterized by unidirectional cross bedding. The thickness is 40 m.

(4) Near the Predmaiskii Creek mouth there are exposed dark gray to black foliated deformed shales with thin (0.5–1.5 cm) siltstone intercalations. Characteristic of the rocks is parallel lamination, sometimes very thin. Transitions between shales and siltstones are either gradual or sharp. Some varieties, e.g., graywackes and micaceous siltstones typical of all exposures of the Burus-Tas Formation, are missing from Member 4. Attitude of beds is distorted by numerous zones of schistosity and boudinage. We got an impression that the member is more intensely deformed, than rocks of members 1–3, because its beds are deformed, for example, into isoclinal folds. All the mentioned features suggest that this member accumulated in different sedimentation environments as compared with underlying sediments. The member separated by a fault from the remaining part of the section does not belong, probably, to the Burus-Tas Formation. Drachev and Savostin, (1993) exclude this member from this formation as well. The apparent thickness is 20–25 m.

Upstream and above the described rocky outcrops, siliciclastic rocks corresponding to lower levels of the Burus-Tas Formation are exposed in places. In the lower course of the left tributary 700 m upstream of the Predmaiskii Creek mouth, there are outcrops of platy

sandstones with irregular lenticular bedding that probably originated under influence of wave activity. The visible lower layers of the section are lithologically similar to rocks considered above. Northward, where dislocation degree of rocks is higher, their sedimentological peculiarities are less distinct.

Taking folding into consideration, the reconstructed thickness of the Burus-Tas Formation in the Predmaiskii creek section is close to 300 m. The described section fragment consists of rocks of relatively shallower origin than sediments of the Cape Burus-Tas area. Its dominant bedded sandstones, cross-bedded varieties included, accumulated probably under influence of tidal currents.

PETROGRAPHY AND MINERAL COMPOSITION

The graywacke type of sandstones became evident already during the field study. As is seen under magnifying glass, sandstones contain a large quantity of feldspar grains and lithoclasts, the latter as abundant as quartz grains or even more. In some beds, there is seen differentiation of clastic material by specific weight: lower parts of these beds are enriched in grains of ore minerals. A characteristic feature of the Burus-Tas Formation in all the examined outcrops is presence of large flakes of detrital white mica. Green sandstones of the Cape Burus-Tas area contain distinct clasts of green rocks and conditionally diagnosed chrysotile flakes of irregular shape up to 2 mm across.

Microscopic examination of sandstones confirms their graywacke composition. Calculation of detrital grains in five representative samples shows that rocks are rich in lithoclasts, which represent approximately a half or even 65% of all the clasts. Feldspar and quartz represent 20–40 and 15–30% of all the identified clasts, respectively (Tables 1, 2). Although the examined five thin sections characterize only some of the rocks, they reflect rather adequately the average composition of dominant sandstones, which are of a monotonous composition in the study area. Some varieties are enriched in quartz grains (up to 50%) or in feldspar clasts prevailing over lithoclasts. Percentage of ore and accessory minerals in basal parts of sandstone interbeds is as

high as 10%. The volume of cement is 25–30%, corresponding approximately to the interstitial space of compacted sand. In the western part of study area, the share of cement is lower because of higher compactness and regeneration of quartz grains. The entire cement is locally replaced here by the chlorite–sericite scaly aggregate.

Quartz grains are usually subangular to angular, acute-angled and wedge-shaped; well-rounded grains occur as well. Grains are mostly represented by monocrystalline quartz with undulatory to less common straight extinction. Polycrystalline quartz grains are subordinate. There are also mosaic quartz aggregates with mutual intergrowth (dominant) of grains and stylolitic sutures. Quartz usually contains scarce gas and gas–liquid inclusions. Intergrowths with other minerals are rare. These are mainly quartz–feldspar intergrowth (granite lithoclasts?). Occasional intergrowths with muscovite, zircon, and apatite are observable as well. These features imply that quartz clasts are derived from metamorphic rocks, granites, and, to a lesser extent, from quartz veins (Simonovich, 1978). Some rounded monocrystalline grains are probably of volcanic origin.

Feldspars are represented by acid plagioclase (albite or, less commonly, oligoclase), usually dull because of secondary alterations. Many grains are lacking polysynthetic twinning. There are also clasts of fibrous or mosaic perthite, which are lacking potassium feldspar according to results of microprobe study: all the examined grains appeared to be composed of albite. Although no thin sections were colored, available observations allow conclusion that the content of K–Na feldspar in sandstones is negligible if it is present at all. Most of plagioclase clasts are likely of volcanic origin. Sometimes, plagioclase crystals are incorporated into recrystallized felsite matrix. Some feldspar clasts originate from granites, as is evident from presence of quartz–feldspar intergrowths.

Muscovite is most widespread among other clasts. Detrital muscovite occurs universally in sandstones of the Burus-Tas Formation sometimes as flakes up to 2 mm across. In green sandstones of the western examined areas, muscovite with greenish tint becomes sometimes green in color. As is seen in thin sections, that coloration is determined by presence of chlorite flakes. Several muscovite and associated chlorite flakes were analyzed (Table 3). Chlorite is compositionally uniform and highly ferruginous. The chlorite–muscovite intergrowths are probably the product of biotite or phengite replacement.

Rocks contain an insignificant quantity of chlorite flakes, hornblende, epidote, and garnet of almandine composition (Table 3). In one of the samples, garnet grains retained the fine sculpture of crystal facets and they look fresh. According to the only analysis, amphibole corresponds in composition to pargasite characteristic of mineral assemblages formed under high pressure and moderately high temperature. The

Table 2. Relative concentrations of components in sandstones of the Burus-Tas Formation (%)

Sample	Q%	F%	L%	Mtx%	Lv	Ls	Lm
135/1	16.5	39.0	44.5	29.5	82.3	15.2	2.3
135/2	26.0	25.6	48.4	29.5	74.8	18.1	6.9
145/8	15.4	20.0	64.6	25.9	78.5	15.1	6.2
146/1	29.0	31.6	39.3	26.1	68.2	10.5	21.1
304/3	21.3	24.6	54.1	29.5	74.5	16.5	8.9

Note: Q% = (Qm + Qp + QF/2)/SUM; F% = (QF/2 + F + P + K)/SUM; L% = (Lv + Ls + Lm + Col + Op)/SUM; Mtx% = Mtx/(Mtx + SUM); Lv = Lv/(Lv + Ls + Lm); Ls = Ls/(Lv + Ls + Lm); Lm = Lm/(Lv + Ls + Lm). For abbreviations, see Table 1.

laboratory study did not confirm presence of serpentine clasts, which were identified visually during field works. Green scaly aggregates appeared to be composed of Cr-chlorite (Table 3), the usual alteration product of orthopyroxene and olivine in mafic rocks. This mineral contains inclusions of high-chromium spinel (Table 3) typical of dunite or harzburgite. Soft shapeless clasts of chlorite could hardly survive the long transport; they are likely derived from serpentinites, similar to those exposed near the Predmaiskii Creek.

Most of lithoclasts are referred to intermediate, acidic, and less common basic volcanics. In most cases, these are microgranular aggregates with plagioclase microlites. Many grains represent aggregates of chlorite, epidote, zoisite, and albite. There are also fragments of porphyritic andesites. In addition, many clasts are represented by the microcrystalline aggregate, which is interpreted as slightly crystallized felsite. Clasts of sedimentary rocks are subordinate, corresponding to cherts, shales, and rare carbonates. Fragments of metamorphic rocks are not numerous, but occur almost in all the samples. They are largely represented by chlorite–sericite schists and quartzites.

Zircon, apatite, and rutile are most widespread accessory minerals. The accessory zircon is represented by crystals highly variable in habit, color, and roundness degree. This is partly explained by its repeated redeposition characteristic of platform settings. Apatite crystals and their fragments are also variable in the shape and roundness degree. One of the samples contains fresh lens-shaped and isometric grains with dissolution signs. Similar crystals were extracted from orthoamphibolites of the southeastern part of Bol'shoi Lyakhov Island, and we consider these rocks as a most probable source of above specific clasts. Rutile, the typical accessory mineral of sedimentary clastic rocks, can be used, along with zircon, as indicator of siliciclastic material maturity (Hubert, 1962). It was suggested that rutile is a cosmopolitan mineral of diverse origin (*Minerals of Sedimentary...*, 1958). It was shown (Force, 1980), however, that the highly metamorphosed rocks only can yield detrital rutile. In the study area, rocks of

Table 3. Chemical composition of some detrital minerals in sandstones of the Burus-Tas Formation

Sample	Mineral	SiO ₂	TiO ₂	Al ₂ O ₃	Cr ₂ O ₃	FeO	MnO	MgO	CaO	Na ₂ O	K ₂ O
303/1	Garnet	41.31		25.05		25.88	2.90	2.90	1.20		
303/1	Garnet	42.59		23.79		26.32	0.90	3.39	2.29		
146/1	Garnet	40.57		23.74		25.49	5.01	3.24	1.83		
303/1	Ilmenite		53.06		0.25	43.73		0.90			
301/3	Ilmenite		53.41			41.95	2.52				
303/1	Chlorite	32.56		28.48		23.90		14.63			
303/1	Chlorite	35.29	0.59	27.65		22.57		12.55			0.57
146/1	Chlorite	32.70		26.69	1.46	26.15		11.76			0.44
146/1	Chlorite	35.50		25.97	1.66	23.75	0.63	9.95			1.63
146/1	Chlorite	32.57		26.57		29.61		12.86			
146/1	Chlorite (in muscovite)	28.45		23.80		36.73		10.22			0.25
146/1	Chlorite (in muscovite)	28.36		24.10		33.75		12.47			
146/1	Chlorite (in muscovite)	26.65		24.96		36.88	0.56	10.35			
146/1	Chlorite (in muscovite)	27.44		24.77		35.32		10.68			0.28
146/1	Muscovite	49.53	0.70	35.41		0.99		1.26		1.00	10.49
146/1	Muscovite	48.05	0.68	36.28		2.24		0.50	0.46	0.58	11.01
304/1	Muscovite	46.91	1.63	37.06		1.64		0.72		0.82	10.71
301/3	Amphibole	45.67		18.19		7.62		15.47	8.98	3.45	0.24
146/1	Chromite (in chlorite)			9.11	59.81	17.15		12.11			

Note: Minerals were determined at the Moscow State University using the electronic microprobe CAMECA Camebax. Blank cells indicate concentrations below the detection limit.

this kind are amphibolites of the Emii-Tas complex characterized by a specific paragenesis of deep-seated origin and containing rutile almost in all rock varieties. One can say with a fair degree of confidence that angular rutile crystals occurring in sandstone samples originate from rocks similar to these amphibolites.

Ore minerals of the Burus-Tas sandstones are mainly represented by ilmenite, subordinate magnetite, and rare chromite. Angular ilmenite fragments are probably derived from rocks similar to the Emii-Tas amphibolites, which universally contain ilmenite, sometimes in concentrations of economic value.

SOURCES OF DETRITAL MATERIAL

The lithoclasts indicate unambiguously that andesites, dacites, and, less commonly, basalts are principal source rocks for sandstones of the Burus-Tas Formation. Such a composition of source rocks points to their island-arc origin, and it is logical to assume that they originated from the Anyui-Svyatoi Nos island arc. Volcanic and comagmatic intrusions could supply also clasts of plagioclase and quartz. Angular long-prismatic colorless small zircon crystals, which were probably brought from the nearby area, also originate presumably from the same source.

The second main source of clastic material is a continental block, the provenance of quartz and erosion

products of granite and metamorphic rocks. A significant share of this clastic material could be subjected to repeated redeposition in sedimentary platform cover before its incorporation into the Burus-Tas graywackes. This is evidenced by rounded zircon grains, which represent a common component of heavy fraction in sandstones of the Burus-Tas Formation. The most probable source of this material is the Paleozoic-Lower Mesozoic sedimentary cover and, probably, metamorphic basement of the New Siberian platform. Detrital mica was likely derived from that platform. Flakes of white mica (muscovite and decomposed biotite) are widespread in sandstones of the Burus-Tas Formation. We undertook an attempt to determine age of mica using the Ar-Ar method. V.A. Ponomarchuk (Joint Institute of Geology, Geochemistry, and Mineralogy, Siberian Division RAS) performed the analysis. The annealing of mica fraction revealed no plateau step and demonstrated gradual increase of radiogenic argon concentration under the temperature growth (Table 4, Fig. 7). Inasmuch as the bulk preparation consisting of many flakes was analyzed, the result obtained is interpreted as characterizing the heterogeneous composition of detrital mica. The heterogeneity can be explained by either the different-age sources, or the non-uniform thermal and/or deformation-related impact on initially coeval mica flakes during their, presumably multiple, burial in sedimentary sequences. The second variant seems more

Table 4. Concentration of Ar isotopes under step heating of detrital muscovite

Step	Age, Ma	$^{40}\text{Ar}/^{39}\text{Ar}$	$^{38}\text{Ar}/^{39}\text{Ar}$	$^{37}\text{Ar}/^{39}\text{Ar}$	$^{36}\text{Ar}/^{39}\text{Ar}$	^{39}Ar , %
1	127.9 ± 5.5	18.9 ± 0.2	0.047 ± 0.0010	0.003 ± 0.0010	0.023 ± 0.0018	9.6
2	285.3 ± 2.1	30.7 ± 0.2	0.025 ± 0.0004	0.002 ± 0.0007	0.008 ± 0.0004	25.2
3	338.2 ± 2.9	36.7 ± 0.3	0.028 ± 0.0004	0.005 ± 0.0002	0.009 ± 0.0005	40.7
4	377.8 ± 3.3	43.4 ± 0.4	0.027 ± 0.0007	0.001 ± 0.0022	0.017 ± 0.0010	50.9
5	432.2 ± 3.2	48.2 ± 0.3	0.025 ± 0.0006	0.006 ± 0.0004	0.012 ± 0.0003	61.2
6	448.4 ± 4.0	50.0 ± 0.3	0.026 ± 0.0005	0.006 ± 0.0007	0.012 ± 0.0009	70.9
7	464.5 ± 2.9	52.2 ± 0.3	0.025 ± 0.0006	0.006 ± 0.0004	0.013 ± 0.0005	80.1
8	474.5 ± 6.0	53.5 ± 0.7	0.028 ± 0.0010	0.008 ± 0.0006	0.014 ± 0.0006	87.5
9	499.3 ± 7.6	55.4 ± 0.5	0.027 ± 0.0019	0.008 ± 0.0008	0.010 ± 0.0022	94.9
10	510.6 ± 4.4	59.5 ± 0.4	0.040 ± 0.0063	0.017 ± 0.0022	0.019 ± 0.0012	98.3
11	529.3 ± 10.7	82.9 ± 0.5	0.073 ± 0.0029	0.013 ± 0.0073	0.090 ± 0.0042	100.0

Note: Analysis is performed in the United Institute of Geology, Geochemistry, and Mineralogy SD RAS, Novosibirsk (analyst V.A. Ponomarchuk).

plausible and indicates the Vendian–Early Paleozoic age of the source. It cannot be ruled out that terranes located in the present-day structure south of the Anyui–Svyatoi Nos arc represented such a source. By the moment of the Burus-Tas Formation deposition, a collage of terranes of northeastern Asia, the continental blocks included, was already amalgamated to a significant extent (Zonenshain *et al.*, 1990; Parfenov *et al.*, 2001).

Ultramafics and, probably, amphibolites were only the subsidiary source of clastic material, though important for determining the tectonic settings. Products of their erosion are chrome spinel and chlorite, and, to some extent, grains of rutile, ilmenite, apatite, and amphibole.

Thus, the mineral composition of siliciclastic rocks of the Burus-Tas Formation suggests that their clastic material originated from several sources: (1) volcanic island arc, (2) ancient platform, and (3) exotic outliers of oceanic and island-arc crust containing serpentinites and amphibolites.

GEOCHEMISTRY OF THE BURUS-TAS FORMATION

The bulk chemical composition is analyzed in 12 samples, and five samples are used to measure trace and rare-earth element concentrations in sandstones of the Burus-Tas Formation (Tables 5, 6). The necessity for geochemical data was not obvious in view of multiple sources of siliciclastic material and probable fractionation of clasts by the specific weight and grain size. In many works, conclusions on the rock composition in provenances and tectonic settings of sedimentation are based on geochemical characteristics of siliciclastic sediments (Argast and Donnelly, 1987; Bhatia, 1983, 1985; Cox and Lowe, 1995; Dinelly *et al.*, 1999; McLennan *et al.*, 1995, and references therein). There-

fore, we decided to use the same approach in this work. As we found, the analyzed rocks are of relatively uniform though specific composition that can be interpreted as presented below.

Major Elements

Before interpretation of chemical composition of the Burus-Tas siliciclastic rocks, it is necessary to estimate to what extent compositional variations are caused by fractionation of detrital material in the course of sedimentation. The degree of such fractionation can be illustrated in variation diagrams similar to the Harker's diagrams used in igneous petrology (Argast and Donnelly, 1987). Variation trends in such diagrams should represent a line of mixing of two or three components. In our case, the main components are: (1) quartz + feldspars + acid lithoclasts, which are poorly fractionated in the course of sedimentation; (2) clay minerals (mainly illite and smectite); (3) minerals of heavy fraction. When the alumina content is taken as the fractionation index, the data points of sandstones and shales form in diagrams two relatively com-

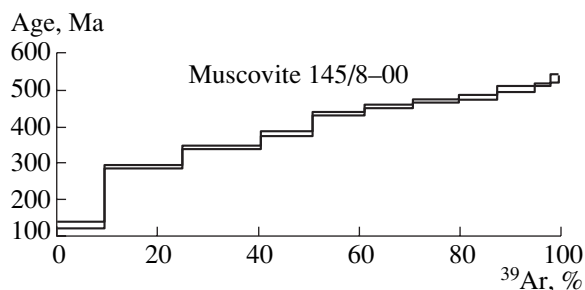


Fig. 7. Plot of the radiogenic argon release under step annealing of detrital muscovite extracted from sandstone (Sample 145/8; Tables 4 and 5).

Table 5. Chemical composition of sandstones and siltstones from the Burus-Tas Formation

Oxide	Sandstone										Argillite			GRW	MP	UC
	135/1	135/2	145/1	145/8	146/1	148/3	205/1	303/1	304/3	ave- rage	146/5	304/4	304/9			
SiO ₂	71.54	71.25	70.14	69.77	73.83	68.49	69.25	65.14	72.88	70.26	58.01	60.89	59.68	69.55	70.04	66.00
TiO ₂	1.03	1.07	0.85	1.02	1.06	1.86	0.93	0.95	0.94	1.08	1.20	1.10	1.17	0.72	0.98	0.50
Al ₂ O ₃	12.94	13.26	14.17	14.12	12.25	13.39	13.16	14.90	13.78	13.55	22.21	20.15	20.85	13.59	15.91	15.20
Fe ₂ O ₃	7.69	7.47	7.88	8.37	6.75	9.21	9.34	12.05	5.88	8.28	8.32	8.62	8.72	5.94	6.67	4.50
MnO	0.12	0.12	0.13	0.13	0.12	0.12	0.14	0.13	0.12	0.13	0.13	0.12	0.12	0.10	0.07	0.10
MgO	2.27	2.19	2.37	2.72	1.84	2.16	3.01	3.47	1.75	2.42	3.44	3.45	3.92	2.32	1.79	2.20
CaO	0.37	0.46	0.34	0.38	0.45	0.61	0.62	0.81	0.49	0.50	0.34	0.37	0.47	2.62	0.43	4.20
Na ₂ O	2.81	2.77	2.41	1.84	2.50	1.91	2.49	1.35	2.14	2.24	1.16	1.82	0.84	3.02	1.11	3.90
K ₂ O	1.09	1.27	1.56	1.50	1.05	2.05	0.90	1.06	1.86	1.37	5.02	3.35	4.05	2.01	2.83	3.40
P ₂ O ₅	0.14	0.13	0.14	0.14	0.14	0.20	0.16	0.15	0.14	0.15	0.19	0.15	0.18	0.13	0.17	
LOI	2.58	2.91	2.81	2.76	2.13	3.50	2.88	3.53	2.38	2.83	4.85	4.48	4.68		3.2	

Note: Results are calculated for 100% "dry" residue composition. (135/1, 135/2) Usuk-Yuryakh River (Fig. 3); (145/1, 145/8, 146/1, 146/5, 148/3) Cape Burus-Tas; (205/1) Pravyi Nerpalakh River; (303/1, 304/3, 304/5, 304/9) Predmaiskii Creek; (GRV) average graywacke after (Wedepohl, 1995); (MP) Millport Graywacke, average for 23 analyses (Argast and Donnelly, 1987); (UC) upper crust (Taylor and McLennan, 1985). Analyses were performed by the X-ray fluorescence method in glassed pills at the United Institute of Geology, Geochemistry, and Mineralogy SD RAS, Novosibirsk.

Table 6. Concentrations of trace and rare earth elements (ppm) in siliciclastic rocks of the Burus-Tas Formation

Element	1	2	3	4	5	6	7
	145/8	146/1	303/1	304/3	304/4	GRW	UC
Sc	19.1	11.5	14.8	12.9	21.1	16	11
V	112	117	133	115	169	98	60
Cr	134	142	118	111	134	88	35
Co	18.4	13.1	20.1	11.7	11.2	15	10
Ni	67.5	47	76.5	42.8	59.8	24	20
Rb	51.9	36.5	35.7	59.2	105	72	112
Sr	57.9	66	155	94.7	85.6	201	350
Y	35.5	27	33.7	33.6	42.2	26	22
Zr	211	213	197	193	257	302	190
Nb	17.2	18.4	17.1	16.4	22	8.4	25
Ba	344	304	251	220	699	426	550
Hf	5.22	5.6	4.92	5.13	6.85	3.5	5.8
Pb	4.38	2.99	6.34	4.26	10.9	14.2	20
Th	10.5	13	9.58	11	15.2	9	10.7
U	2.72	2.85	2.39	2.72	3.9	2	2.8
La	28.1	21.9	25.6	30.5	40	34	30
Ce	63	50.1	58	66.6	80.9	58	64
Pr	7.85	6.3	7.24	7.92	9.74	6.1	7.1
Nd	31.1	24.3	29.4	31.4	37.3	25	26
Sm	6.35	4.79	5.99	6.07	7	4.6	4.5
Eu	1.42	1.1	1.45	1.53	1.38	1.2	0.88
Gd	5.54	4.19	5.82	5.72	6.17	4	3.8
Tb	0.884	0.725	0.917	0.877	1.05	0.63	0.64
Dy	5.1	4.3	5.21	5.24	6.21	3.4	3.5
Ho	1.16	1	1.17	1.17	1.48	0.78	0.8
Er	2.85	2.65	2.98	3.07	4.06	2.2	2.3
Tm	0.438	0.415	0.463	0.468	0.624	nd	0.33
Yb	2.86	2.73	2.75	2.89	4.18	2.1	2.2
Lu	0.405	0.403	0.414	0.442	0.616	0.37	0.32
Th/Sc	0.55	1.13	0.65	0.85	0.72	0.56	0.97

Note: (1–4) sandstones; (5) argillite; (6) average graywacke after (Wedepohl, 1995); (7) model composition of the upper crust (Taylor and McLennan, 1988). The analysis was performed by the ICP-MS method at the Institute Mineralogy and Geology of Rare Elements. See also note to Table 5.

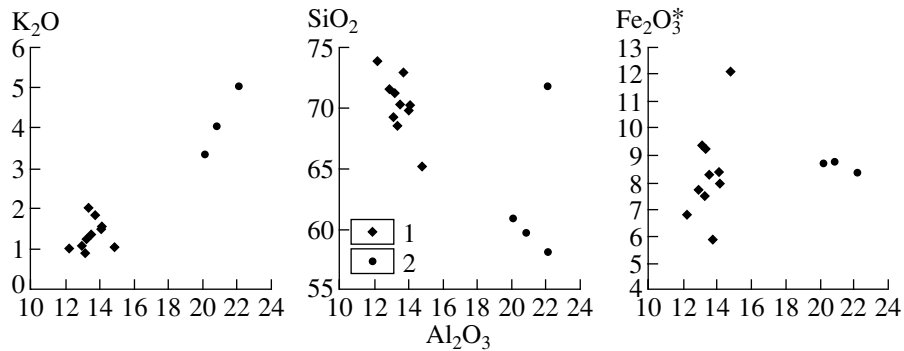


Fig. 8. Variation diagrams for siliciclastic rocks of the Burus-Tas Formation: (1) sandstones; (2) shales .

compact isolated clusters between end members of variation series (Fig. 8). This indicates that chemical variations of the Burus-Tas sandstones mainly reflect the bulk composition of clastic material in provenances, being controlled by fractionation of mineral grains in the course of sedimentation to insignificant extent only.

The first peculiarity to be noted is high TiO_2 (0.85–1.86% averaging 1.05%) and $Fe_2O_3^*$ (5.88–12.05% averaging 8.28%) concentrations in sandstones that is inconsistent with relatively high alumina content. The measured values substantially exceeding those typical of graywackes accumulated in different geodynamic settings (Bhatia, 1983). As we believe, the obvious cause is a high content of detrital ore minerals such as rutile, ilmenite, titanomagnetite, and magnetite derived largely from ophiolites and amphibolites of the Bol'shoi Lyakhov Island. The second characteristic feature is the extremely low CaO content (0.34–0.81% averaging 0.50%) in the Burus-Tas sandstones. This can be explained by CaO removal from the provenance in the course of chemical weathering and also from sediments during the early diagenesis (Cox and Lowe, 1995; Argast and Donnelly, 1987). The assumption is supported by relatively low Na_2O content in sandstones, because this soluble component could be readily leached either from the source rocks or by diagenesis of sediments. Graywackes with similarly low CaO concentrations are described from several areas. An appropriate example is the Millport Sandstone of the Rainstreet Formation of the New York State (Argast and Donnelly, 1987). Average values characterizing 23 rock samples from the above unit are presented in Table 5. The relevant molasses accumulated during the Acadian orogeny in prodelta–open-shelf settings. Judging from petrographic description, these rocks contain abundant detrital plagioclase despite low concentrations of CaO and Na_2O (Argast and Donnelly, 1987).

Bhatia (1983) proposed to use the following parameters for classifying and comparing chemical compositions of sandstones: $Fe_2O_3^* + MgO$; TiO_2 ; Al_2O_3/SiO_2 ; K_2O/Na_2O ; $Al_2O_3/(CaO + Na_2O)$. Distinct differences

in these parameters were revealed by statistical processing of chemical data obtained for sandstones accumulated in different tectonic settings. The above parameters are selected based on the following arguments. In sedimentogenesis, Fe and Ti are immobile elements, and Mg can be used, despite its substantially higher mobility, because of rapid burial of sediments in the course of siliciclastic sedimentation. At the same time, the Al_2O_3/SiO_2 ratio is indicative of sandstone enrichment in clastic quartz, while the K_2O/Na_2O value characterizes the relation between plagioclase, on the one hand, and feldspar and layered silicates, on the other (Bhatia, 1983). The $Al_2O_3/(CaO + Na_2O)$ ratio is useless in our case because of extremely low $CaCO_3$ concentration, which is untypical of graywackes. In many works, the K_2O/Na_2O value is used to identify volcanogenic sources of clastic material: when $K_2O/Na_2O < 1$, the role of volcanogenic material in graywackes is significant, whereas $K_2O/Na_2O > 1$ signifies contribution of continental source to sandstone formation (McLennan *et al.*, 1990; Bock *et al.*, 1998). According to Bhatia's diagrams (Fig. 9), the Burus-Tas graywackes could be accumulated in island-arc settings as is evident from $Fe_2O_3 + MgO$ and TiO_2 concentrations. On the other hand, these sediments may be composed of material from continental island arcs, as one can judge from Al_2O_3/SiO_2 and K_2O/Na_2O parameters. In any case, the data obtained reflect a high concentration of volcanoclastic material in the Burus-Tas graywackes and point to a significant role of the Anyui–Svyatoi Nos island arc in supplying the Burus-Tas basin with clastic material.

Trace Elements

Concentrations of trace elements in four sandstone and one shale samples are relatively uniform (Table 6). This averaging of geochemical characteristics can probably be explained by repeated redeposition of material and insignificant fractionation of heavy minerals, such as zircon, rutile, garnet, ilmenite, and others, which are main concentrators of trace elements. In

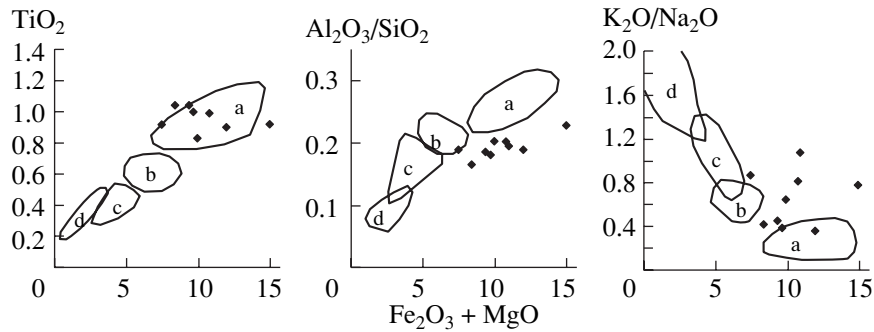


Fig. 9. Discrimination diagrams based on proportions of rock-forming oxides (Bhatia, 1983) with fields outlining (a) oceanic settings, (b) continental arcs, (c) active continental margins, (d) passive continental margins.

shales, concentrations of trace elements, including the least mobile ones (Sc, Th, Zr, Hf, REE, and others) are slightly higher than in sandstones, probably because they are sorbed to clay minerals, on the one hand, whereas sterile quartz is present in sandstones, on the other (Cox and Lowe, 1995; McLennan *et al.*, 1990).

As compared with standard graywackes, siliciclastic rocks of the Burus-Tas Formation have higher Cr (128 ppm on average) and Ni (59 ppm on average) concentrations (Table 6). This implies presence of ultramafic rocks in the provenance.

Sediments of the Burus-Tas Formation are also characterized by relatively high contents of heavy REE and Y concentrated usually in garnet and, to a lesser extent, in amphiboles and pyroxenes. They are enriched as well in Nb, an element usually concentrated in standard accessory minerals of granite and in rutile. The accessory minerals could be also derived from metamorphic rocks, e.g., from amphibolites of the Emii-Tas type. Acidic metamorphites and granites are less appropriate candidates for the Nb source, otherwise sediments would have elevated Zr concentrations in this case.

According to McLennan *et al.* (1990), the Th/Sc ratio is a sensitive indicator of the provenance compo-

sition. In their opinion, these elements do not participate in processes of hypergenesis, being buried in siliciclastic sediments during deposition. Sc is a constituent of carbonate sedimentary minerals in rocks (Dinelly *et al.*, 1999), but this factor can be ignored in the case of the Burus-Tas sandstones. The Th/Sc ratio in examined rocks is highly variable, being usually lower than in the average crust, thus indicating a substantial contribution of the volcanogenic source (McLennan *et al.*, 1990).

Rare Earth Elements

The REE spectra in siliciclastic sediments are considered as the most objective and informative tool for identifying the type of the source of clastic material and tectonic aspects of sedimentation settings (Bhatia, 1985; Taylor and McLennan, 1988). The REE distribution is uniform in examined samples (Fig. 10). In the shale, the REE content is slightly higher as compared with that in sandstones. This situation is typical of turbidites (McLennan *et al.*, 1995) and relevant causes have been discussed earlier. Characteristic of the Burus-Tas siliciclastic rocks are the relative flat distribution patterns of heavy REE ($Gd(n)/Yb(n) = 1.5$ on average), a moderate Eu anomaly ($Eu/Eu^* = 0.73$ on average), and moderate fractionation degree of light REE ($La(n)/Sm(n) = 3.1$ on average). In these parameters of the REE spectra, the Burus-Tas sediments are strikingly similar to the model composition of the upper crust (Taylor and McLennan, 1988) and to standard average compositions of siliciclastic rocks such as common graywacke (Wedepohl, 1987) (Table 6) or post-Archean shale of Australia (Taylor and McLennan, 1988). Similar REE distribution patterns are also typical of standard andesite (Taylor and McLennan, 1988). In general, the Burus-Tas siliciclastic sediments differ from standard compositions mentioned above in a slightly lower degree of general REE fractionation ($La(n)/Yb(n) = 6.8$) and somewhat higher concentrations of heavy REE (Table 6). This difference can be interpreted as pointing to notable admixture of material from sources with poorly differentiated REE (tholeiites) and/or substantial content of minerals concentrat-

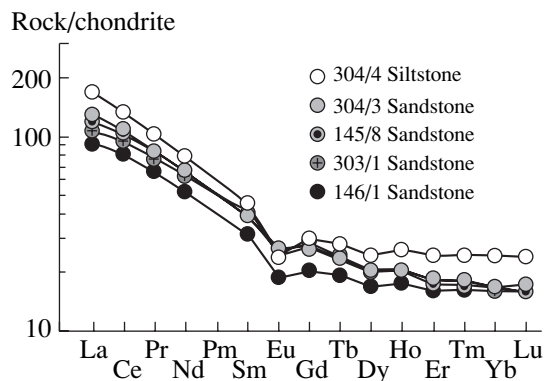


Fig. 10. REE distribution in siliciclastic rocks of the Burus-Tas Formation (normalizing chondrite values after Taylor and McLennan, 1988).

ing heavy REE, e.g., of garnet, in the composition of heavy fraction.

Summing up, we can conclude the following.

(1) Chemical composition of the Burus-Tas siliciclastic sediments suggests a substantial influx in sedimentation basin of clastic material derived from volcanics. (2) Erosion of igneous mafic and ultramafic rocks also influenced significantly the chemical composition of sediments in question. (3) Clayey and sandy sediments originate from the same sources.

These inferences show that geochemical study of sedimentary rocks reveals some peculiarities in their composition, which cannot be disclosed by petrographic studies. It is of interest that geochemical data demonstrate a strikingly uniform composition of examined rocks, although significant dispersion in concentrations of elements could be expected judging from mineralogical and petrographic criteria: we specially analyzed rocks, which are most different in terms of rock-forming and accessory minerals.

AGE OF THE BURUS-TAS FORMATION

The petrographic, mineral, and chemical compositions of rocks from the Burus-Tas Formation imply that their clastic material is dominated by erosion products of volcanic island arc (1) and of continental basement (?) and its sedimentary cover subjected to recycling (2); serpentinites and amphibolites (3) represented a supplementary source. We assume that rocks of the Anyui-Svyatoi Nos arc represented the first source; rocks of the New Siberian platform formed the second one. The third source corresponded to allochthonous tectonic wedges and nappes similar to those exposed now in the southeastern part of Bol'shoi Lyakhov Island, where they are composed of ophiolite rocks and amphibolites. The simultaneous contribution of these three sources to sedimentary infill of the Burus-Tas basin suggests that the latter originated at the time of collision between the Anyui-Svyatoi Nos arc and New Siberian platform. We assume also that volcanism in the Anyui-Svyatoi Nos arc ceased during accumulation of siliciclastic sediments after closure of the Anyui ocean, when fragments of oceanic lithosphere were exhumed to the erosion level. These events are dated ambiguously within the time span from the terminal Jurassic to mid-Neocomian (Natal'in, 1984; Parfenov, 1984; Zonenshain *et al.*, 1990; Sokolov *et al.*, 2002). They lasted probably some time. Volcanics of the Cape Svyatoi Nos area are correlated with the Oxfordian-Kimmeridgian, while in the South Anyui area, Lower Cretaceous volcanics are developed as well (Parfenov *et al.*, 2001). Based on indirect evidence (see below), we believe that the Anyui ocean closed entirely at the end of the Jurassic. This assumption is consistent with biogeographic data. Zakharov *et al.* (2002) demonstrated that a barrier, which separated previously the Siberian and Canadian zoogeographic provinces, disappeared in the terminal Jurassic. It is assumed that the deep Anyui ocean, which

closed at that time, served as a barrier. It cannot be ruled out that calc-alkaline magmatism could be in progress for some time after the collision commencement.

Consequently, the lower age limit of syncollision sediments cannot be older than the terminal Jurassic. The upper age limit for these sediments can be determined based on discordant granites that intrude the Burus-Tas Formation. The most reliable Ar-Ar date obtained for biotite from postcollision granodiorites in the southeastern part of Bol'shoi Lyakhov Island corresponds to the Aptian (114.4 ± 0.5 Ma, Layer *et al.*, 2001). Thus, the Burus-Tas Formation age should be in the range of the terminal Jurassic-Neocomian. The syncollision molasse in the South Anyui area is of a similar ages (Bondarenko *et al.*, 2003). Based on these indirect data, we assume that Permian-Triassic age previously suggested for the Burus-Tas Formation is derived from redeposited organic remains and cannot characterize the sedimentation period.

We attempted to determine the lower age limit of the Burus-Tas Formation using the fission-track method to disclose the youngest generation of detrital zircons. Assuming that acidic and intermediate volcanics of the Anyui-Svyatoi Nos arc were source rocks of siliciclastic influx into the Burus-Tas basin, one should expect that sediments of the formation contain the Jurassic generation of zircons. The heavy fraction from sandstones of the Burus-Tas Formation contains fresh long prismatic colorless zircon crystals, which could originate from this source.

Zircon fractions of two sandstone samples from the Cap Burus-Tas area were analyzed by the fission-track method. Both samples contain zircons of variable color, habit, and preservation degree. The method is described in a series of works (Brandon and Vance, 1992; Garver *et al.*, 2000; Bondarenko *et al.*, 2003). A short etching time and observed fission-track populations of different ages suggest that zircons have not been overheated after their precipitation and retain information about the initial age of the fission-track system closure in provenance (approximately 200°C). We dated 40 zircon grains per each sample. Information about older populations has not been obtained, because we omitted special treatment of samples with a shorter etching period of zircon preparations.

The counted fission tracks show that both samples contain the same zircon population close in age to 160 Ma (163.7 ± 9.3 and 159.0 ± 23.8 Ma; Fig. 11). We assume that these zircons have been derived from the Anyui-Svyatoi Nos arc containing the Oxfordian calc-alkaline andesites, basalts, and comagmatic diorites (Parfenov *et al.*, 2001). In addition, Sample 146/1 contains the zircon population that is 119.6 ± 14.5 (1 σ) Ma old. This population consists largely of euhedral crystals, but its age is too young to be a result of magmatic activity in the Svyatoi Nos arc. The following interpretations of its origin are admissible.

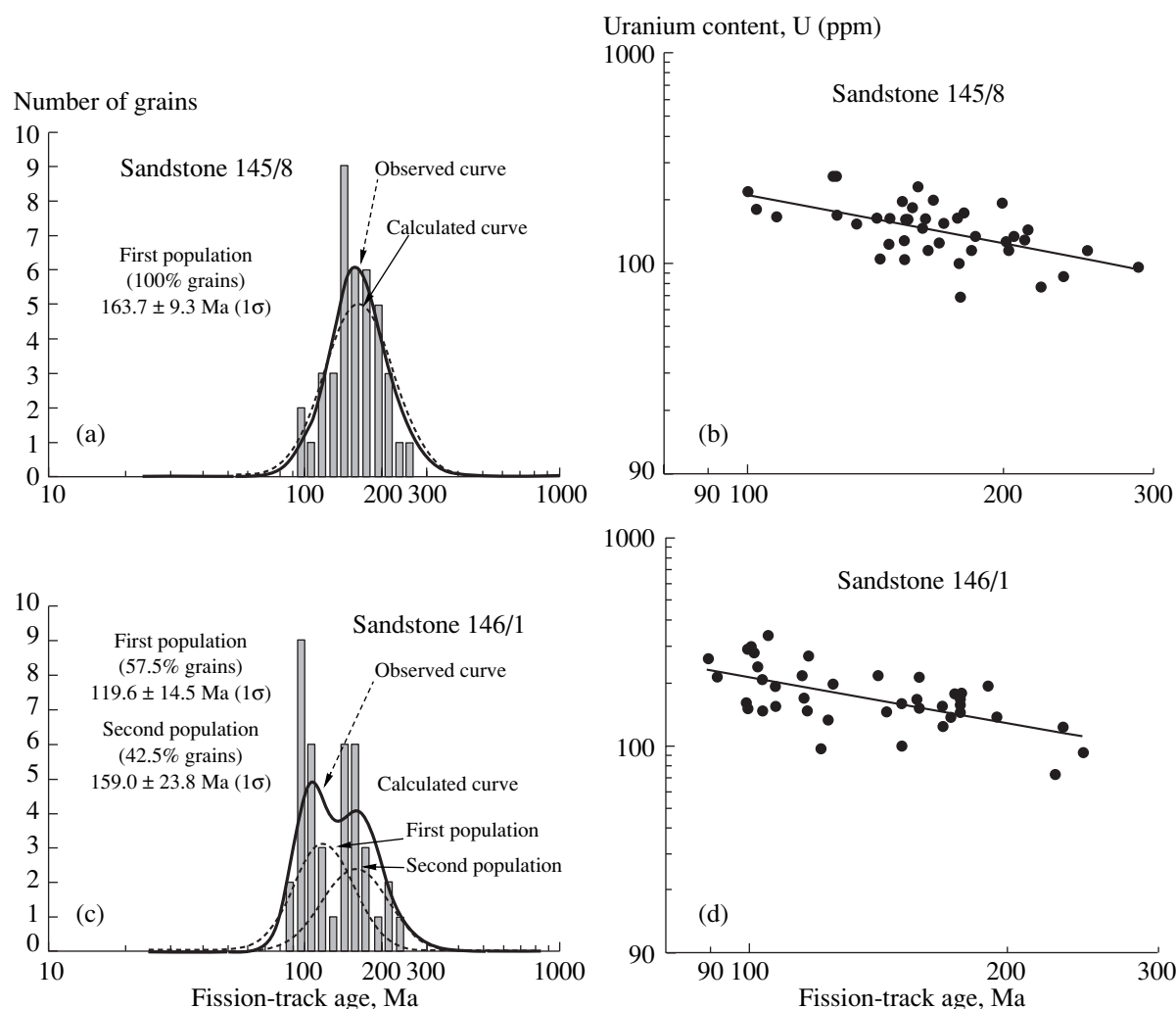


Fig. 11. Distribution of fission-track ages obtained for detrital zircon grains from sandstones of the Burus-Tas Formation (a, b); programs Zetaage 4.7 and Binomfit 1.8 (Brandon, 2002) are used to calculate ages of individual zircon grains and analysis of distribution of ages. Dependence of fission-track ages on uranium concentration in zircon grains (c, d); sampling sites are shown in Fig. 5 and analyses are performed at the laboratories of the mineralogical and fission-track analysis of the Geological Institute RAS and Union College (Schenectady, New York, USA).

(1) The obtained date corresponds to volcanic activity in a remote provenance. In the Chukchi Peninsula for instance, there are acidic calc-alkaline lava and tuffs of Neocomian age, which are thought to be connected with magmatism in the Oloi arc (Parfenov *et al.*, 2001; Sokolov *et al.*, 2001).

(2) Zircons could originate from rock complexes exhumed to the erosion level during terminal orogenic phases. In this case, the population age reflects the moment of complex intersection with the isotherm of 200°C. Taking into consideration the lower confidence limit, the above age value is within the range expected for deposition of the Burus-Tas Formation, which accumulated, as is shown above, synchronously with orogenic processes.

(3) The population is close in age to the nearby granite-granodiorite massif (114.4 ± 0.5 Ma. Layer *et al.*,

2001) that means a possibility of secondary annealing of zircons. According to fission-track dating, Sample 146/1 contains several zircon populations different in age. This indicates usually that zircons escaped secondary annealing. There are, however, examples of rocks containing several zircon populations and grains, some with fission tracks subjected to secondary annealing and the other ones lacking such tracks (Hasebe *et al.*, 1993; Garver *et al.*, 2004). A situation like this is assumed to be characteristic of rocks, which resided for a relatively long period within a zone, where thermal regime is close to the reset temperature of the fission-track system (about 200°C) for zircons, and rocks, therefore, contain zircons characterized by different properties and different degree of track annealing (Garver *et al.*, 2004). Zircon properties that control the fission-track annealing are poorly studied, although it is known that the uranium concentration is one of the

main influencing factors, and tracks in high-uranium zircons are first subjected to annealing. In the fission-track age–uranium content diagram, data points of annealed grains usually form an autonomous cluster showing no linear correlation with other zircons (Garver *et al.*, 2004). The distribution of data points of Sample 146/1 in the diagram is inappropriate for a confident assessment of secondary annealing, although it indicates that the population aged 119.6 ± 14.5 Ma is characterized in terms of statistics by higher U concentrations (Fig. 11d). We cannot exclude a partial secondary annealing, because sandstones from the Cape Burus-Tas area contain newly formed chlorite and sericite, which suggests a thermal impact on rocks. In order to solve the problem under consideration, we plan to date using fission-track method the zircons from the Predmaiskii Creek section, where rocks are substantially less altered, and/or to determine the U–Pb age of zircons, because the closure temperature of this isotopic system is significantly higher.

Thus, the results of fission-track dating show that the Burus-Tas sandstones contain the Middle–Late Jurassic zircon population. The fission-track age of this population corresponds to the closure time of the track system in the source of clastic material. Zircon could originate in igneous rocks of the Anyui–Svyatoi Nos island arc and in rocks heated once to the temperature exceeding 200°C and exhumed to the upper crustal levels in the Middle–Late Jurassic. In addition, Sample 146/1 contains zircons with the Early Cretaceous population of fission tracks. The age interpretation of this population is ambiguous and does not exclude a possibility of secondary annealing of zircons in sedimentary rocks.

The direct evaluation of the lower age limit of the Burus-Tas Formation is well consistent with all the indirect data indicating that siliciclastic sediments of the formation accumulated since the Late Jurassic only. This inference is supported by data on age of siliciclastic flysch sequences in the Stolbovoi and Malyi Lyakhov islands (Stolbovoi Formation). The Late Jurassic (Volgian)–Early Cretaceous (Berriasian–Valanginian) age of the Stolbovoi Formation is substantiated by bivalves. Sandstones of the Stolbovoi Formation represent graywackes lithologically similar to their counterparts in the Burus-Tas Formation (Voronkov, 1958; Vinogradov and Yavshits, 1975; Vol'nov *et al.*, 1999; Dorofeev *et al.*, 1999; *Placer Deposits...*, 2001). The Late Jurassic–Neocomian siliciclastic complex is also widespread in the South Anyui area, where it is composed of shales and graywackes enclosing conglomerates with pebbles of serpentinites, oceanic and island arc volcanics (Natal'in, 1984; Bondarenko *et al.*, 2003). Thus, we can conclude that all siliciclastic flyschoid sequences of the Bol'shoi Lyakhov Island constitute a single stratigraphic unit of the Late Jurassic (Volgian)–Early Cretaceous (Berriasian–Valanginian) age determined by analogy with paleontologically substantiated sequences of Stolbovoi Island. It cannot be ruled out

that the Burus-Tas Formation includes younger Neocomian strata missing from the Stolbovoi island section.

TECTONIC ORIGIN OF SEDIMENTARY BASIN

The obtained data on composition of the Burus-Tas Formation rocks and their sedimentological peculiarities suggest that they accumulated in a foredeep that appeared on the southern margin of the New Siberian continental block during its collision with the Anyui–Svyatoi Nos arc. It is believed that relevant sedimentary basins appeared in front of the moving orogen in response to compensatory subsidence of the crust. The studied fragments of the siliciclastic sequence are inappropriate for distinguishing sediments of different basin areas and/or different stages in sedimentation. The bottom of sedimentation basin was locally influenced by storm waves, i.e., the basin was several tens of meters deep (Dott and Bourgeois, 1982). Co-occurrence of beds with graded bedding and hummocky cross stratification is characteristic of facies of the flood-dominated deltaic systems (Mutti *et al.*, 2003). It is assumed that suspended siliciclastic material was transported from a mountainous provenance by numerous small and medium-sized rivers during floods. The mass transport of suspended material to the sea gave birth to bottom hyperpycnal flows, which could spread over a large distance to deposit sediments with graded bedding. The stormy weather accompanied by intense atmospheric precipitation was responsible for influx of sandy–silty material and its deposition in a form of cross bedded successions (Mutti *et al.*, 2003).

We assume that clastic material was transported to the Burus-Tas basin from an orogen located southerly. This structure was composed of rocks corresponding to (1) island arc volcanics and comagmatic intrusions, (2) exhumed wedges that belonged formerly to the southern margin of the New Siberian platform, and to (3) exotic blocks that included fragments of the South Anyui oceanic lithosphere and basement rock complexes of the island arc (Fig. 12). Erosion of orogen with such an intricate structure, which was thrust over the margin of the New Siberian platform, could provide simultaneously clastic material from all the identified sources.

Wedges composed of exotic rocks, the oceanic pillow lavas, island arc metagabbro, subduction-related glaucophane schists, and serpentinites included, are observable at the present-day surface. Being subjected to erosion, they turn into provenance of serpentinite clasts lacking signs of long-distance transport. These clasts are detected in sandstones containing simultaneously the rounded “recycled” zircons. It is possible as well that in distribution areas of the Burus-Tas Formation there are tectonic wedges of Triassic shales detached from the southern passive margin of the New Siberian platform. The black shale member exposed in the Predmaiskii Creek area (Fig. 6), the specific composition of which was noted by Drachev and Savostin

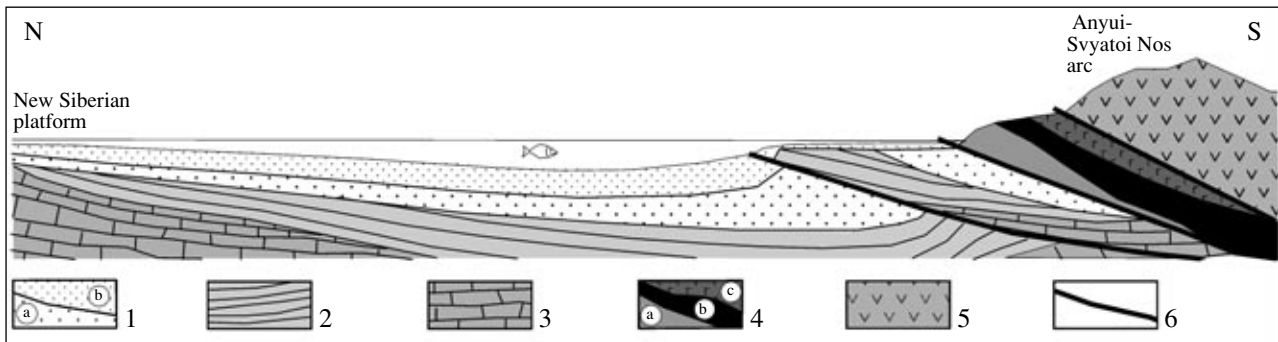


Fig. 12. Schematic model of the syncollision Volgian–Neocomian Burus-Tas basin and orogen of intricate structure thrust over the margin of the New Siberian platform; model illustrates the late stage of the basin infill formation, when sediments of the earlier stage were partly included into the orogenic structure: (1) siliciclastic sequences of the foredeep (J_{3v} – K_{1nc}): (a) early stage, (b) later stage; (2) siliciclastic sequences of the New Siberian platform passive margin (T–J); (3) sedimentary cover of the New Siberian platform (Pz_{2-3}); (4) tectonic wedges of oceanic rocks and subduction-related metamorphic rocks: (a) serpentinites, (b) pillow basalts, (c) amphibolites and glaucophane schists; (5) rocks of the Anyui–Svyatoi Nos arc (J); (6) thrusts.

(1993), can be one of the wedges. This could explain an enigmatic find of the Middle Triassic bivalve near the Predmaiskii Creek mouth. The opinion of A.B. Aulov (private communication) that Triassic shales occur along the northern front of the South Anyui suture from the Chukchi Peninsula to Bol'shoi Lyakhov Island seems quite reasonable. In the South Anyui region, Triassic and Neocomian siliciclastic rocks are exposed in the same areas, and their discrimination during geological survey is difficult (Sokolov *et al.*, 2002; Bondarenko *et al.*, 2003). We think that the Triassic autochthon is unexposed in the present day structure of Bol'shoi Lyakhov Island, but allochthonous slices of Triassic shales can be present in the packets of tectonic nappes thrust over the southern margin of the New Siberian platform (Fig. 12). The orogen could include also slices of Permian siliciclastic rocks of the platform cover. Their erosion and redeposition could be responsible for occurrence of coal clasts with Permian spores–pollen assemblages in the Burus-Tas Formation rocks. Permian and Triassic siliciclastic sequences proper are composed of material derived from the New Siberian platform, and during redeposition, they could be the main source of continental clastic material.

The simplified model outlined above is a satisfactory explanation of the Burus-Tas Formation composition, although the real situation could be significantly more complex. By the beginning of the Cretaceous, the intricate Kolyma–Omolon orogenic structure that comprised, in addition to the Anyui–Svyatoi Nos arc, fragments of different-age island arcs and continental blocks, the Omolon massif included, already existed in the rear of the Anyui–Svyatoi Nos island arc (Parfenov *et al.*, 2001; Sokolov *et al.*, 2002). This rear part of the orogen was probably responsible for the influx of mixed clastic material into the Burus-Tas basin.

Thus, we think that the Burus-Tas Formation is the Late Jurassic–Early Cretaceous in age, i.e., coeval with siliciclastic sequences exposed in northern and western

parts of the Bol'shoi Lyakhov Island. It should be noted that previous finds of organic remains in the Burus-Tas Formation seem logical in the context of our model.

Within the study area, the Burus-Tas basin was in direct contact with the orogen, because proximal facies are missing from the visible section of the Burus-Tas Formation. At the present-day surface, the Burus-Tas Formation encloses tectonic slices of serpentinites and pillow basalts. Apparently, their tectonic juxtaposition occurred likely after accumulation of examined fragments of the siliciclastic complex. Consequently, these rocks correspond to relatively early stages of the foredeep formation.

CONCLUSIONS

(1) Lithological, mineral, and chemical compositions of siliciclastic rocks exposed in southeastern areas of the Bol'shoi Lyakhov Island suggest three provenances of clastic material: (a) a volcanic island arc, (b) ancient platform, and (c) exotic detached block composed of serpentinites and amphibolites. The inferable composition of provenances implies that clastic sediments accumulated at the time of collision between the continental block of the New Siberian shelf and southerly located Anyui–Svyatoi Nos island arc. Sediments of the examined sections accumulated in the flood-dominated deltaic settings. The syncollision basin accumulated clastic material transported from the orogenic structure thrusting from the south.

(2) Siliciclastic sediments exposed in southeastern areas of the Bol'shoi Lyakhov Island are the Late Jurassic (Volgian)–Early Cretaceous (Neocomian) in age. The lower age limit is determined by precollision Oxfordian–Kimmeridgian (Parfenov *et al.*, 2001) volcanics of the Anyui–Svyatoi Nos island arc that participated in collision and supplied clastic material to the syncollision foredeep basin. The Middle–Late Jurassic (approximately 160 Ma) age of zircon population

present in sandstones of the Burus-Tas Formation is confirmed by fission-track dating. The upper age limit is determined as corresponding to the Aptian (114.4 ± 0.5 Ma), when discordant postcollision granites intruded siliciclastic rocks. We assume that tectonic wedges of Triassic sedimentary rocks, which accumulated on the passive margin of the New Siberian platform, are present among Volgian–Neocomian rocks exposed in the southeastern part of the island. The former idea that siliciclastic sequence of the Bol'shoi Lyakhov Island is Permian in age seems to be based on redeposited organic remains.

(3) We propose to unite siliciclastic sequences exposed in the northern, western, and southeastern parts of Bol'shoi Lyakhov Island into a single complex of Mesozoic (Volgian–Neocomian) rocks, i.e., to accept the initial interpretation. Siliciclastic complexes of similar age, composition, and tectonic position are described in the Stolbovoi and Malyi Lyakhov islands and in the South Anyui area. All these sequences are exposed north of the South Anyui suture and accumulated in one foredeep.

ACKNOWLEDGMENTS

We are grateful to V.A. Ponomarchuk for the Ar–Ar analysis of muscovite, D.Z. Zhuravlev for the analysis of trace elements, and to V.A. Zakharov and S.D. Sokolov for reviewing the manuscript and valuable comments. This work was supported by the Russian Foundation for Basic Research (project no. 05-05-64028), Program “Leading Scientific Schools” of the Russian Federation (grant NSh-1980.2003.5) and INTAS (grant 01-0762 NEMLOR). Fission-track dating of zircon grains was supported by the Foundation for the Support of Russian Science, Program of Fundamental Research of the Branch of Earth Sciences RAS, and American Foundation for Civil Research and Development for independent countries of the former Soviet Union (grant CRDF no. RG1-2568-MO-03).

Reviewers V.A. Zakharov
and S.D. Sokolov

REFERENCES

1. S. Argast and T. W. Donnelly, “The Chemical Discrimination of Clastic Sedimentary Components,” *Sediment. Petrology* **57**, 813–823 (1987).
2. M. R. Bhatia, “Plate Tectonics and Geochemical Composition of Sandstones,” *J. Geol.* **91**, 611–627 (1983).
3. M. R. Bhatia, “Rare Earth Element Geochemistry of Australian Paleozoic Graywackes and Mudrocks: Provenance and Tectonic Control,” *Sedimentary Geol.* **45**, 997–1130 (1985).
4. B. Bock, S. M. McLennan, and G. N. Hanson, “Geochemistry and Provenance of the Middle Ordovician Austin Glen Member (Normanskil Formation) and the Teacon Orogeny in New England,” *Sedimentology* **45**, 635–655 (1998).
5. G. E. Bondarenko, A. V. Soloviev, M. I. Tuchkova, *et al.*, “Age of Detrital Zircons in Sandstones of the Upper Mesozoic Flysch Formation in the South Anyui Suture Zone (Western Chukotka),” *Litol. Polezn. Iskop.* **38** (2), 1–17 (2003) [*Lithol. Mineral Resources* **38**, 162–177 (2003)].
6. M. T. Brandon, “Decomposition of Mixed Grain–Age Distribution Using BINOMFIT,” *On Track* **24**, 13–18 (2002).
7. M. T. Brandon and J. A. Vance, “Tectonic Evolution of the Cenozoic Olympic Subduction Complex, Western Washington State, as Deduced from Fission Track Ages for Detrital Zircon,” *Amer. J. Sci.* **292**, 565–636 (1992).
8. R. Cox and D. R. Lowe, “A Conceptual Review of Regional-scale Controls on the Composition of Clastic Sediment and the Co-evolution of Continental Blocks and Their Sedimentary Cover,” *J. Sediment. Res.* **A65** (1), 1–12 (1995).
9. E. Dinelly, F. Luccini, A. Mordenty, and L. Paganelly, “Geochemistry of Oligocene–Miocene Sandstones of the Northern Apennines (Italy) and Evolution of Chemical Features in Relation to Provenance Changes,” *Sedimentary Geol.* **127**, 193–207 (1999).
10. V. K. Dorofeev, M. G. Blagoveshchenskii, A. N. Smirnov, and V. I. Ushakov, “New Siberian Islands, Geological Structure and Mineral Assemblages,” Ed. by V. I. Ushakov (VNIIOkeangeologiya, St. Petersburg, 1999) [in Russian].
11. R. H. Dott and J. Bourgeois, “Hummocky Stratification: Significance of Its Variable Bedding Sequences,” *Geol. Soc. Amer. Bull.* **93**, 663–680 (1982).
12. S. S. Drachev and L. A. Savostin, “Ophiolites of Bol'shoi Lyakhov Island (New Siberian Islands),” *Geotektonika*, No. 3, 98–107 (1993).
13. G. Einsele, *Sedimentary Basins. Evolution, Facies, and Sediment Budget* (Berlin, Springer, 1992).
14. M. M. Ermolaev, “Geologic and Geomorphologic Essay on the Bol'shoi Lyakhov Island,” in *Polar Geophysical Station on Bol'shoi Lyakhov Island. Part I. Organization and Work of the Station in 1927–1930* (AN SSSR, Leningrad, 1932), pp. 147–228 [in Russian].
15. E. R. Force, “The Provenance of Rutile,” *J. Sediment. Petrology* **50**, 485–488 (1980).
16. N. Hasebe, T. Tagami, and S. Nishimura, “Evolution of the Shimanto Accretionary Complex: A Fission-Track Thermochronologic Study,” in *Thermal Evolution of the Tertiary Shimanto Belt, Southwest Japan: An Example of Ridge–Trench Interaction*, Ed. by M. B. Underwood (Geol. Soc. Amer., Boulder, 1993), pp. 121–136.
17. A. F. Hubert, “A Zircon–Tourmaline–Rutile Maturity Index and the Interdependence of the Composition of Heavy Mineral Assemblages with the Gross Composition and Texture of Sandstones,” *J. Sediment. Petrol.* **32**, 440–450 (1962).
18. J. I. Garver, A. V. Soloviev, M. E. Bullen, and M. T. Brandon, “Towards a More Complete Record of Magmatism and Exhumation in Continental Arcs, Using Detrital Fission-Track Thermochronometry,” *Phys. and Chemist. Earth* **25**, 565–570 (2000).

19. J. I. Garver, A. V. Soloviev, and P. W. Reiners, "Field Observations of the Stability of Fission Tracks in Radiation-Damaged Zircon," in *10th International Fission Track Conference. Abstr. Volume* (2004), p. 56.
20. P. W. Layer, R. Newberry, K. Fujita, *et al.*, "Tectonic Setting of the Plutonic Belts of Yakutia, Northeast Russia, Based on $^{40}\text{Ar}/^{39}\text{Ar}$ Geochronology and Trace Element Chemistry," *Geology* **29**, 167–170 (2001).
21. S. M. McLennan, S. R. Taylor, M. T. McCulloch, and J. B. Maynard, "Geochemical and Nd–Sr Isotopic Composition of Deep-sea Turbidites: Crustal Evolution and Plate Tectonic Associations," *Geochim. Cosmochim. Acta* **54**, 215–250 (1990).
22. "Minerals of Sedimentary Rocks," in *Guidebook to Petrography of Sedimentary Rocks. Volume I. Formation Conditions, Properties, and Minerals of Sedimentary Rocks* (Gosnauchtekhizdat, St. Petersburg, 1958), pp. 190–414 [in Russian].
23. E. Mutti, R. Tinterri, G. Benevelli, *et al.*, "Deltaic, Mixed, and Turbidite Sedimentation of Ancient Forland Basins," *Marine and Petroleum Geol.* **20**, 733–755 (2003).
24. B. A. Natal'in, *Early Mesozoic Eugeosynclinal Systems in the Northern Part of the Circum-Pacific Belt* (Nauka, Moscow, 1984) [in Russian].
25. B. A. Natal'in, J. M. Amato, J. Toro, J. E. Wright, "Paleozoic Rocks of Northern Chukotka Peninsula, Russian Far East: Implications for the Tectonics of the Arctic Region," *Tectonics* **18**, 977–1003 (1999).
26. L. M. Parfenov, *Continental Margins and Island Arcs of Mesozooids in Northeastern Asia* (Nauka, Novosibirsk, 1984) [in Russian].
27. L. M. Parfenov, V. S. Oksman, A. V. Prokop'ev, *et al.*, "Collage of Terranes in the Verkhnyaya Kolyma Orogenic Region," in *Tectonics, Geodynamics, and Metallogeny of the Sakha Republic Territory*, Ed. by L. M. Parfenov and M. I. Kuz'min (Nauka/Interperiodika, Moscow, 2001), pp. 199–255 [in Russian].
28. *Placer Deposits of the Lyakhov Tin-bearing Area*, Ed. by I.S. Gramberg and V.I. Ushakov (VNIIOkeangeologiya, St. Petersburg, 2001) [in Russian].
29. A. I. Samusin and K. N. Belousov, *State Geological Map of the SSSR (Scale 1: 200000. New Siberian Island Series. Sheets S-53-XVI, XVII, XXIII; S-54-XIV–XVI, XX–XXVII, XXVII–XXX. Explanatory Notes*, Ed. by A.M. Ivanova (Soyuzgeolfond, Moscow, 1985) [in Russian].
30. K. B. Seslavinskii, "South Anyui Suture (Western Chukotka)," *Dokl. Akad. Nauk SSSR* **249**, 1181–1185 (1979).
31. I. M. Simonovich, *Quartz of Sedimentary Rocks* (Nauka, Moscow, 1978) [in Russian].
32. S. D. Sokolov, G. Ye. Bondarenko, O. L. Morozov, *et al.*, "The South Anyui Suture: Facts and Problems to Solve," in *Tectonic Evolution of the Bering Shelf–Chukchi Sea–Arctic Margin and Adjacent Landmasses*, Ed. by E. L. Miller, S. Klemperer, and A. Grantz (Geol. Soc. Amer. Spec. Paper 360, 2000), pp. 209–224.
33. S. R. Taylor and S. M. McLennan, *The Continental Crust, Its Composition, and Evolution* Blackwell, Oxford, 1985; Mir, Moscow, 1988).
34. V. A. Vinogradov, A. F. Dibner, and A. I. Samusin, "On Discrimination of Permian Sediments in Bol'shoi Lyakhov Island," *Dokl. Akad. Nauk SSSR* **219**, 1200–1202 (1974).
35. V. A. Vinogradov and G. P. Yavshits, "Stratigraphy of Upper Jurassic and Lower Cretaceous Sediments in Northern Areas of the Stolbovoi Island," in *Geology and Mineral Resources of the New Siberian Islands and Wrangel Island* (NIIGA, Leningrad, 1975), pp. 38–42 [in Russian].
36. D. A. Vol'nov, V. N. Voitsekhovskii, O. A. Ivanov, *et al.*, "The New Siberian Islands," *Geology of the USSR. Volume 26. Islands of the Soviet Arctic Region, Geological Description*, Ed. by B.V. Tkachenko and B.Kh. Egiyazarov (Nedra, Moscow, 1970), pp. 324–374 [in Russian].
37. D. A. Vol'nov, B. G. Lopatin, D. S. Sorokov, *et al.*, *State Geological Map of the Russian Federation. Scale 1: 000000 (New Series). Sheet S-53-55 – New Siberian Islands. Explanatory Notes* (VSEGEI, St. Petersburg, 1999) [in Russian].
38. V. N. Voitsekhovskii and D. S. Sorokov, "Precambrian Rocks of the Bol'shoi Lyakhov Island (New Siberian Islands)," *Inform. Byull. NIIGA, Issue 4*, 4–7 (1957).
39. K. A. Volossovich, "On Geological Works in the New Siberian Islands Report on Works of the Russian Polar Expedition Headed by Baron E Toll," in *Notes Emperor Acad. Sci.* **16**, 240–243 (1901).
40. A. V. Voronkov, "Geological Structure of the Stolbovoi Island, New Siberian Archipelago," in *Geology of the Soviet Arctic Region. New Siberian Islands* (NIIGA, Leningrad, 1958), pp. 37–43 [in Russian].
41. K. H. Wedepohl, "The Composition of the Continental Crust," *Geochim. Cosmochim. Acta* **59**, 1217–1232 (1995).
42. V. A. Zakharov, B. N. Shurygin, N. I. Kurushin, *et al.*, "Mesozoic Ocean in the Arctic Region: Paleontological Evidence," *Geol. Geofiz.* **43** (2) 155–181.
43. L. P. Zonenshain, M. I. Kuz'min, and L. M. Natapov, *Plate Tectonics of the USSR Territory* (Nedra, Moscow, 1990), Book 2 [in Russian].